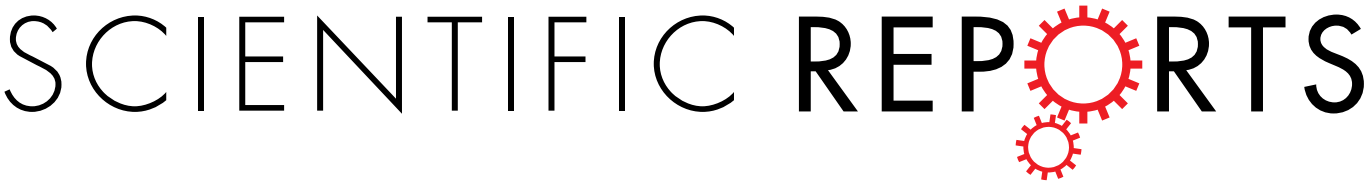

OPEN

Theoretic Study on Dispersion Mechanism of Boron Nitride Nanotubes by Polynucleotides

Received: 22 August 2016
Accepted: 28 November 2016
Published: 22 December 2016

Lijun Liang[1,*], Wei Hu[2,*], Zhisen Zhang[3] & Jia-Wei Shen[4]

Due to the unique electrical and mechanical properties of boron nitride nanotubes (BNNT), BNNT has been a promising material for many potential applications, especially in biomedical field. Understanding the dispersion of BNNT in aqueous solution by biomolecules is essential for its use in biomedical applications. In this study, BNNT wrapped by polynucleotides in aqueous solution was investigated by molecular dynamics (MD) simulations. Our results demonstrated that the BNNT wrapped by polynucleotides could greatly hinder the aggregation of BNNTs and improve the dispersion of BNNTs in aqueous solution. Dispersion of BNNTs with the assistance of polynucleotides is greatly affected by the wrapping manner of polynucleotides on BNNT, which mainly depends on two factors: the type of polynucleotides and the radius of BNNT. The interaction between polynucleotides and BNNT(9, 9) is larger than that between polynucleotides and BNNT(5, 5), which leads to the fact that dispersion of BNNT(9, 9) is better than that of BNNT(5, 5) with the assistance of polynucleotides in aqueous solution. Our study revealed the molecular-level dispersion mechanism of BNNT with the assistance of polynucleotides in aqueous solution. It shades a light on the understanding of dispersion of single wall nanotubes by biomolecules.

Nanotubes, especially carbon nanotubes, due to their unique mechanical and electronical properties, have been extensively investigated in last two decades[1–4]. Although the chemistry of carbon nanotubes (CNTs) has correspondingly been developed to extend their applicability, there are still many stubborn problems blocking the way toward the real applications of CNTs[5]. In this respect, boron nitride nanotubes (BNNTs) made from BN nanosheet are much more attractive due to their special physicochemical properties[6–13]. As a counterpart of a CNT, BNNT possesses notably higher chemical stability and resistance to oxidation[14,15], whereas it exhibits very similar mechanical properties and thermal conductivity[16]. The most interesting thing is that BNNTs are transparent to visible light due to its constant wide band gap (around 5.2–5.8 eV)[17–19]. In addition, Ciofani *et al.* revealed that BNNT has a good cytocompatibility in living cell[20,21]. These studies greatly enhanced our understanding on the properties of BNNTs. They show that BNNTs could be used in many potential applications especially nano-biomedical application[22–27].

To realize these promising application of BNNTs, the aggregation of BNNTs in the aqueous needs to be overcome[28]. In potential applications, dispersion of BNNTs with the assistance of biomolecules is a good choice due to the natural property of biomolecules. Especially, the isolation of BNNTs with the assistance of peptides has been successfully achieved in experiment[29]. Moreover, theoretical studies showed that DNA and polynucleotides has strong interactions with BNNTs[30,31]. These studies give a strong hint on the dispersion of BNNT in aqueous with the assistance of DNA or polynucleotides molecules. However, understanding the dispersion mechanism of BNNT by DNA and polynucleotides in aqueous is essential but still unclear. It could give a guideline on the dispersion of single-walled nanotubes by biomolecules. In addition, it could also provide an insight on the fundamental understanding of interaction between biomolecules and nanomaterials.

[1]College of Life Information Science and Instrument Engineering, Hangzhou Dianzi University, Hangzhou, People's Republic of China. [2]Division of Theoretical Chemistry and Biology, School of Biotechnology, KTH Royal Institute of Technology, SE-10691 Stockholm, Sweden. [3]Research Institute for Biomimetic and Soft Matter, Fujian Provincial Key Laboratory of Soft Functional Materials, Department of Physics, Xiamen University, Xiamen, 361005, People's Republic of China. [4]School of Medicine, Hangzhou Normal University, Hangzhou 310016, People's Republic of China. *These authors contributed equally to this work. Correspondence and requests for materials should be addressed to Z. Z. (email: zhangzs@xmu.edu.cn) or J.W.S. (email: shen.jiawei@hotmail.com)

System	BNNT	Radius of BNNT (nm)	polynucleotides	Atoms	Simulation time (ns)
MD simulations					
BNNT(9, 9)-A_{15}	Single BNNT(9, 9)	0.620	A_{15}	63, 559	20
BNNT(9, 9)-T_{15}	Single BNNT(9, 9)	0.620	T_{15}	63, 544	20
BNNT(9, 9)-C_{15}	Single BNNT(9, 9)	0.620	C_{15}	63, 559	20
BNNT(9, 9)-G_{15}	Single BNNT(9, 9)	0.620	G_{15}	63, 592	20
MBNNT(9, 9)	9 BNNT(9, 9)	0.620	/	194, 084	100
MBNNT(9, 9)-A_{15}	9 BNNT(9, 9)	0.620	A_{15}	252, 212	100
MBNNT(9, 9)-T_{15}	9 BNNT(9, 9)	0.620	T_{15}	252, 917	100
MBNNT(9, 9)-C_{15}	9 BNNT(9, 9)	0.620	C_{15}	253, 049	100
MBNNT(9, 9)-G_{15}	9 BNNT(9, 9)	0.620	G_{15}	252, 674	100
BNNT(5, 5)-A_{15}	Single BNNT(5, 5)	0.345	A_{15}	35, 567	20
BNNT(5, 5)-T_{15}	Single BNNT(5, 5)	0.345	T_{15}	35, 585	20
BNNT(5, 5)-C_{15}	Single BNNT(5, 5)	0.345	C_{15}	35, 546	20
BNNT(5, 5)-G_{15}	Single BNNT(5, 5)	0.345	G_{15}	35, 564	20
MBNNT(5, 5)-A_{15}	9 BNNT(5, 5)	0.345	A_{15}	213, 745	100
MBNNT(5, 5)-T_{15}	9 BNNT(5, 5)	0.345	T_{15}	214, 871	100
DFT calculations					
BNNT(9, 9)-A		Single BNNT(9, 9)		A	
BNNT(9, 9)-T		Single BNNT(9, 9)		T	
BNNT(5, 5)-A		Single BNNT(5, 5)		A	
BNNT(5, 5)-T		Single BNNT(5, 5)		T	

Table 1. The details of performed systems in this study.

Besides experiments, molecular dynamics (MD) simulation has been successfully used to investigate the interaction between biomolecules and nanotubes[32–39]. MD simulation could provide comprehensive understanding at the atomic level. Recently, Liang *et al.* revealed the insertion process of CNTs into DNA nanotubes by mean of MD simulation[34]. Shen *et al.* found that the chirality of CNTs could greatly affect the interaction between CNTs and polynucleotides[36]. Moreover, density functional theory (DFT) calculations could describe more detailed structures between DNA and CNTs.

Based on this background, MD simulations combined with DFT calculations were used to investigate the interaction between polynucleotides and BNNTs in this study. To investigate the effect of nucleotide type on the dispersion of BNNTs, different types of single strand of polynucleotides including poly$(A)_{15}$, poly$(T)_{15}$, poly$(C)_{15}$ and poly$(G)_{15}$ (abbreviated as A_{15}, T_{15}, C_{15} and G_{15} in the following of this paper) were used to represent polynucleotides. The details of simulations are listed in the Table 1. Our simulations demonstrate that the BNNT wrapped with polynucleotides could well disperse in aqueous solution and the aggregation of BNNTs could be hindered.

Computational Methods

Molecular dynamics simulation. The armchair (5, 5) and (9, 9) BNNTs were constructed by visual molecular dynamics (VMD) tool[40]. The diameters of them are 0.69 nm and 1.24 nm with the length of 5.00 nm, respectively. The vertical axis of two BNNTs is along *z* direction. Polynucleotides including A_{15}, T_{15}, C_{15} and G_{15} were constructed by Hyperchem (Version 7.0, Hypercube, Inc)[41], and they were equilibrated for 10 ns in MD simulation in vacuum. After that, polynucleotides were immersed into the water box with size of $8.0 \times 8.0 \times 10\,nm^3$, and certain number of Na^+ ions was added into the water box to neutralize the system. Then 10 ns MD simulation in *NpT* ensemble was performed to equilibrate the system. The structure of polynucleotides at the final state of the equilibration was exacted as the initial structure for investigating the interaction between BNNTs and polynucleotides. The vertical axis of the BNNTs surface was selected to be parallel to the *z*-direction, hence the cross sections of the BNNTs are in the *x*–*y* plane. Then the equilibrated polynucleotides were placed on the top of the BNNTs with the vertical axis of polynucleotides parallel to the vertical axis of BNNTs, and the distance between the center of mass (COM) of polynucleotides and the surface of BNNTs is around 2.0 nm. TIP3P water molecules[42] were added into the box with system density of $1.002\,g/cm^3$. The number of water molecules is slightly different in different system, and the details are displayed in Table 1. At last, Na^+ ions were added into the solution to neutralize the system. In most cases, the water box is $8.00 \times 8.00 \times 10.00\,nm^3$ in the *x*, *y* and *z* directions, as shown in Fig. 1.

After the wrapping process of polynucleotides on single BNNTs, the complexes including BNNTs and polynucleotides were used as the initial structure to investigate the effect of polynucleotides on the aggregation process of BNNTs. 9 BNNT-polynucleotides complexes were copied in *x-y* plane. After that, they were immersed into the water box, and around 81, 200 water molecules were added into the box. At last, Na^+ ions were added into the water box to neutralize the system. The system of 9 BNNT(9, 9)-poly$(A)_{15}$ complexes contains 251, 212 atoms including water molecules, and the total number of atoms in different systems containing MBNNTs is slightly different in different systems, as shown in Table 1.

The polynucleotides, Na^+ and Cl^- ions were modeled by the Charmm27 force field[43]. The force field parameters of boron atoms and nitride atoms in BNNTs were taken from the reference[44]. The charge on N atoms is $-0.3e$,

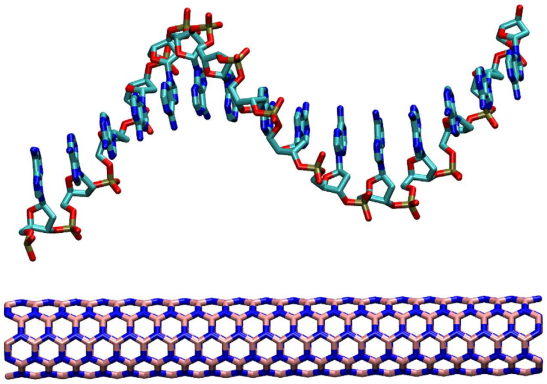

Figure 1. Initial structure for BNNTs (5, 5) with a single strand of poly(A)$_{15}$ from the side view. The polynucleotides molecule and BNNTs are shown by licorice model. The water molecules and ions are not shown for clarity.

and it is 0.3*e* on B atoms. All atoms including hydrogen atoms were represented explicitly, and the bonds with hydrogen atom were constrained by LINCS algorithm. The non-bonded van der Waals interaction was set by a switching function starting at 1.0 nm and reaching zero at 1.2 nm. The Particle mesh Ewald (PME) summation[45] was used to calculate the long-ranged electrostatic interactions, with a cutoff distance of 1.2 nm for the separation of the direct and reciprocal space. All simulations were performed by Gromacs-4.6.3 program with the time step of 2 fs. Periodic boundary conditions (PBC) were applied in all MD simulations. After energy minimization and 10 ns equilibration, all MD simulations were carried out in *NpT* ensemble, and the Langevin method was employed to keep the temperature at 298 K and the pressure at 101.3 kPa, respectively.

Density functional theory calculations. All DFT calculations were performed using PBC model implemented in the Vienna ab initio simulation package (VASP)[46]. The projector augmented wave pseudopotentials were employed to represent the interaction between the core ions and the valence electrons[47]. Meanwhile, the exchange-correlation effects were mainly described by the Perdew−Burke−Ernzerhof generalized-gradient approximation (GGA-PBE)[48], with a plane-wave basis cutoff of 400 eV. To consider the Van der Walls interaction between nucleotides and BNNT, DFT-D3 method with Becke-Jonson damping was used[49]. The structures of different nucleotides adsorbed on BNNT with different radius were first optimized. The interaction energy between nucleotides and BNNT was defined as:

$$\Delta E = E_{sub} + E_{nuc} - E_{sub+nuc} \quad (1)$$

where E_{sup} represents the energy of BNNT, E_{nuc} and $E_{sub+nuc}$ represents the energy of the nucleotides and the complexed system (eg. nucleotide + BNNT), respectively. To avoid the contribution of the preparation energy, E_{sub} and E_{nuc} were calculated from the restricted geometries which were extracted from the corresponding structures of the optimized complexed systems[50].

Results and Discussion

Wrapping of polynucleotides around BNNTs. The distance between center of mass of polynucleotides and the center of mass of BNNT (9, 9) was measured and displayed in Fig. 2. Herein, to investigate the packing manner of polynucleotides on BNNT (9, 9), only the *x* and *y* components in the center of mass were calculated. As shown in Fig. 2, the distance between COM of all different polynucleotides to the surface BNNT (9, 9) decreases in the simulation. The distance between G_{15} and BNNT(9, 9) is about 0.91 nm, and it is around 1.03 nm between C_{15} and BNNT(9, 9). Especially, the distances from A_{15} and E_{15} to the surface of BNNT(9, 9) are both less than 0.2 nm. It shows that all polynucleotides could adsorb on BNNT (9, 9) surface. The packing manner of polynucleotides including A_{15}, T_{15}, C_{15} and G_{15} on the BNNT (9, 9) were observed in the simulation. As seen in Fig. 3, the wrapping conformation of polynucleotides on the BNNT (9, 9) was extracted after 20 ns simulation. A_{15} and T_{15} could tightly surrounded the BNNT (9, 9), as seen in Fig. 3a and b. As shown in Fig. 3c and d, C_{15} and G_{15} can also adsorb on BNNT (9, 9) but only part of BNNT (9, 9) was tightly surrounded by C_{15} or G_{15}. It implies that the wrapping manner of different polynucleotides on BNNT (9, 9) is different. The wrapping of A_{15} and T_{15} on BNNT(9, 9) is much better than C_{15} and G_{15}. It was confirmed by the adsorption number of bases and angle of polynucleotides on BNNT(9, 9) from the last 5 ns simulation. Herein, the adsorption base was defined as: distance between COM of one base and the surface of BNNT(9, 9) is less than 6.0 Å, as described in our previous work[51]. The angle is calculated between the base plane of polynucleotides and *x*-*y* plane of BNNT(9, 9). As seen in Fig. 4, the number of adsorbed bases of A_{15} and T_{15} on BNNT(9, 9) is more than that of C_{15} and G_{15} on BNNT(9, 9). The angle between bases of A_{15} and T_{15} and BNNT(9, 9) is larger than that of C15 and G15. It implicated that the bases of A_{15} and T_{15} is more favorable to adopt the orientation that parallel to the BNNT (9, 9), comparing to the bases of C_{15} and G_{15}. It confirmed that the bases of A_{15} and T_{15} tend to stack on the surface of BNNT (9, 9). In addition, as seen in Fig. 3, all the bases are closely adsorbed on the surface of BNNT(9, 9), and the phosphate

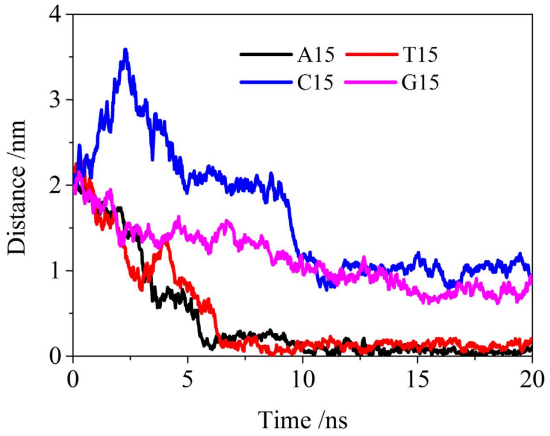

Figure 2. The distance between the center of mass of polynucleotides (A_{15}, T_{15}, C_{15}, and G_{15}) and the surface of single BNNT(9, 9) in *x-y* plane.

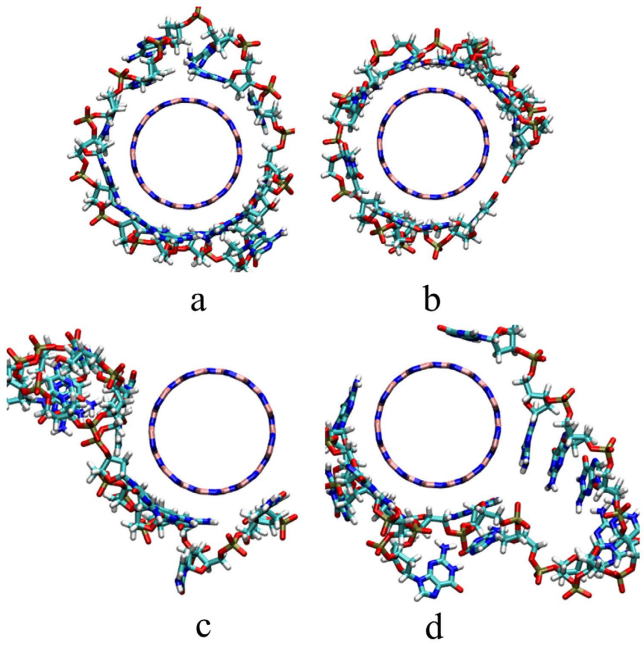

Figure 3. The wrapping conformation of polynucleotides on BNNT(9, 9) at the end of simulation. (**a**) A_{15}; (**b**) T_{15}; (**c**) C_{15} and (**d**) G_{15}.

groups are arranged to be far away from the surface of BNNT(9, 9). The adsorption behaviors of polynucleotides on BNNT(9, 9) is quite similar to that of polynucleotides on neutral carbon nanotubes (CNTs)[35].

To understand the wrapping manner of polynucleotides on BNNT(9, 9) more deeply, the density of phosphorus atoms around BNNT (9, 9) in *x-y* plane from the last 5 ns simulation was measured. The density of phosphorus atoms of polynucleotides in *x-y* plane is along the surface of BNNT(9, 9). Especially, the shape of density distribution of phosphorus atoms is quite similar to the shape of BNNT(9, 9) in *x-y* plane in systems with A_{15} (Fig. 5a) and T_{15} (Fig. 5b). There is only one layer of phosphorus atoms distributed on the surface of BNNT(9, 9) in the systems with A_{15} or T_{15}. It implicated that BNNT(9, 9) is tightly surrounded by A_{15} or T_{15}, and all the bases of A_{15} or T_{15} interacted strongly with BNNT(9, 9). For the system with C_{15} (Fig. 5c) or G_{15} (Fig. 5d), the BNNT(9, 9) was also tightly surrounded by part of polynucleotides but not the whole polynucleotides. Therefore, the interaction between the rest polynucleotides and BNNT(9, 9) is relatively weak due to the unpacked interaction manner.

To better understand the dispersion mechanism of BNNT by polynucleotides, the density of phosphorus and oxygen atoms in phosphate group, nitride atoms in base to the surface of BNNT(9, 9) was measured, as shown in Fig. 6. The first peak of nitride atoms is about 0.35 nm to the surface of BNNT(9, 9), and it is about 0.60 nm of phosphorus atoms to the surface of BNNT(9, 9) in all systems. It reveals that the base of polynucleotides but not phosphate groups is adsorbed on the surface of BNNT(9, 9) in all systems. It implicated that pi-pi interaction

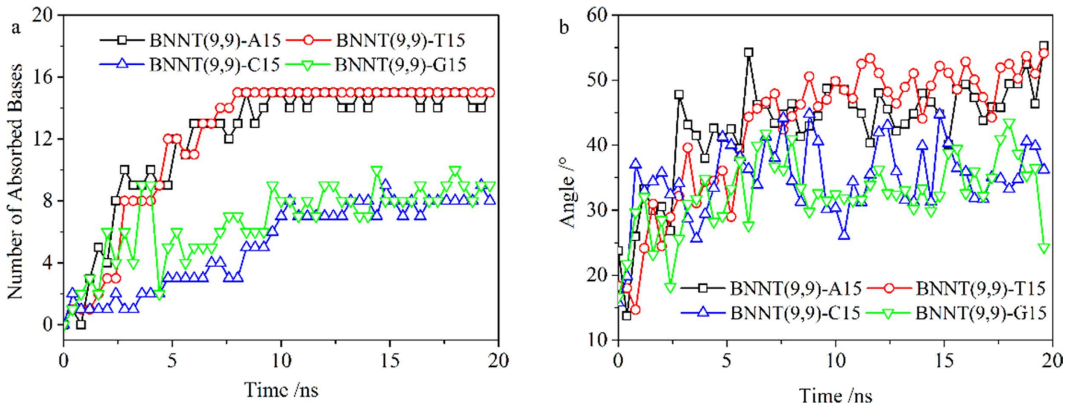

Figure 4. (**a**) The number of adsorbed bases of polynucleotides (including A_{15}, T_{15}, C_{15} and G_{15}) on BNNT(9, 9) as a function of simulation time. (**b**) The averaged angle between bases of polynucleotides and the *x-y* plane of BNNT(9, 9) with respect to simulation time.

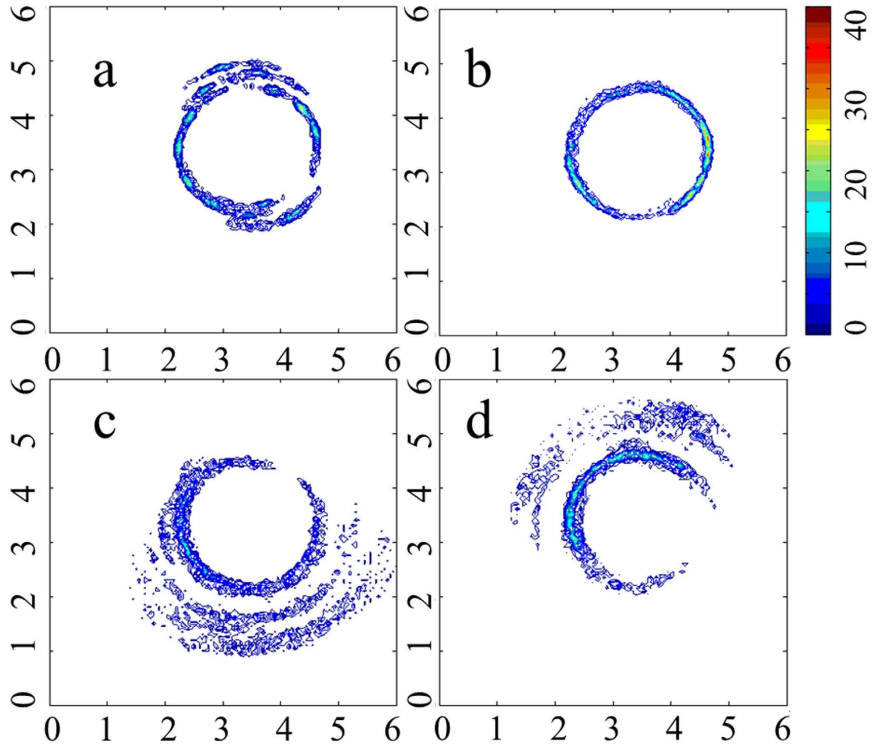

Figure 5. Density of phosphorus atoms of polynucleotides around BNNT (9, 9) in *x-y* plane. (**a**) A_{15}; (**b**) T_{15}; (**c**) C_{15}; (**d**) G_{15}.

between bases and BNNT(9, 9) is important for the adsorption of polynucleotides on BNNT(9, 9), and the phosphate groups were relatively far from the surface of BNNT(9, 9). The adsorption behavior of polynucleotides on BNNT(9, 9) is similar to the adsorption behavior of polynucleotides on CNT (10, 10)[48]. Similar to adsorption of polynucleotides on neutral CNT (10, 10), the adsorption of polynucleotides also relies on the base of polynucleotides on positively charged boron atoms and negatively charged nitride atoms. To investigate the importance of van der Waals (vdW) interaction on adsorption of polynucleotides on BNNT(9, 9), the interaction between BNNT(9, 9) and different polynucleotides from the last 5 ns simulation were measured, as shown in Fig. 7. Herein, the total interaction between polynucleotides and BNNT(9, 9) was divided into two parts: vdW interaction and electrostatic (Ele) interaction. The percentages of vdW interaction are more than 90% in all systems. Moreover, the change of both vdW and electrostatic interaction during last 5 ns in MD simulation in these systems were displayed in Figure S1. These results implicated that the vdW interaction is most important interaction between polynucleotides and BNNT(9, 9).

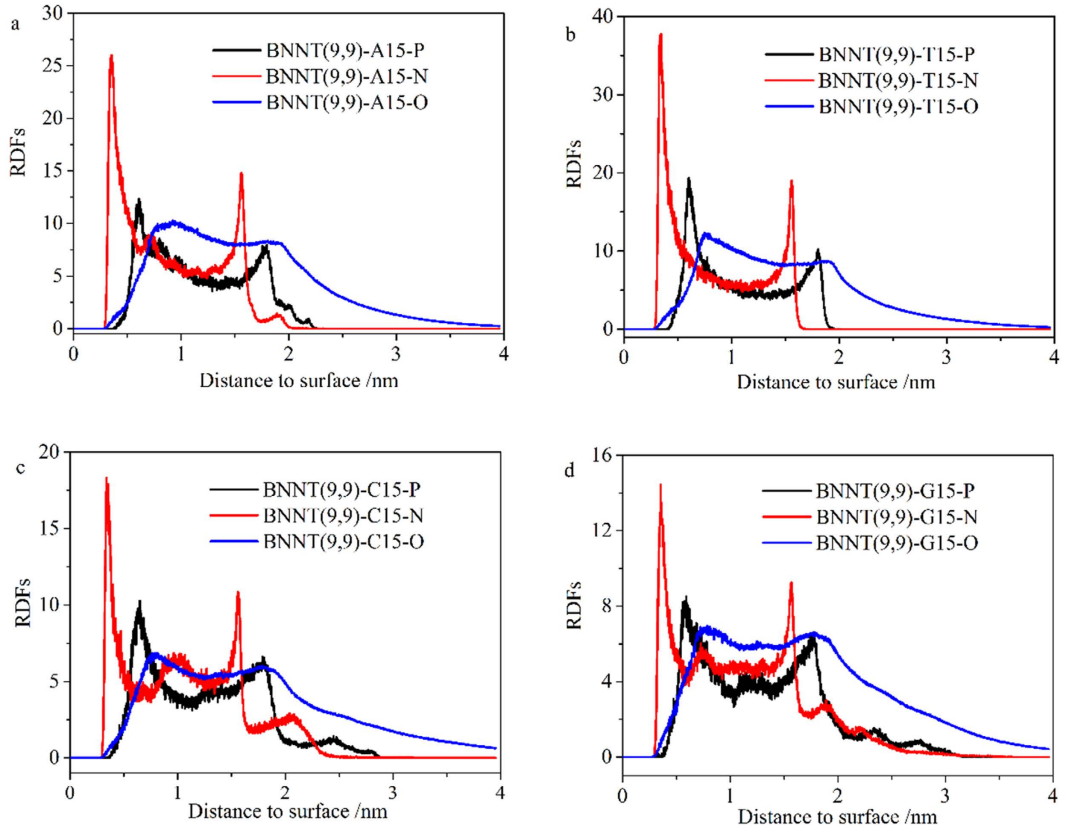

Figure 6. Density of phosphorus atoms and oxygen atoms in phosphate group and nitride atoms in base on the x-y plane of BNNT(9, 9) in different systems: (**a**) A_{15}; (**b**) T_{15}; (**c**) C_{15} and (**d**) G_{15}.

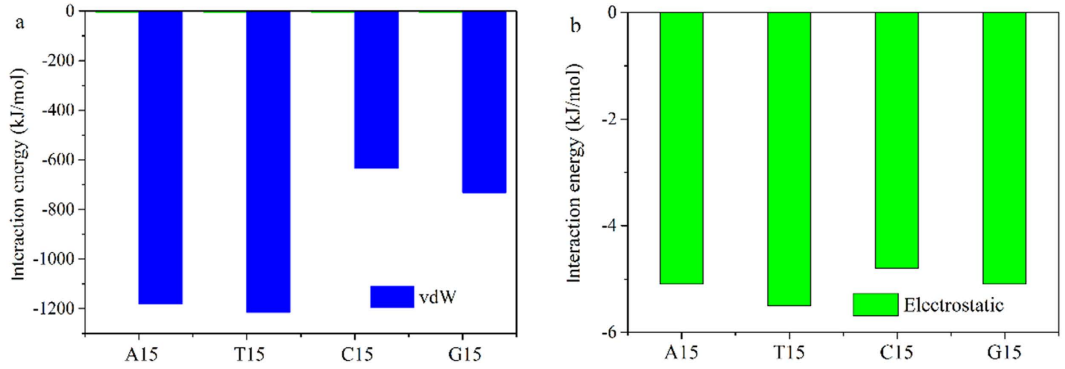

Figure 7. The interaction energy between polynucleotides and BNNT(9, 9): (**a**) vdW interaction energy (blue) and (**b**) electrostatic interaction energy (green).

Dispersion of multiple BNNTs. To investigate the effect of polynucleotides on the dispersion of BNNT(9, 9) in aqueous solution, the simulations (details in Table 1) including 9 BNNT(9, 9) with or without polynucleotides were performed. The number of cluster in different systems with respect to the simulation time is measured, as shown in Fig. 8. The multiple BNNT(9, 9) without polynucleotides could aggregated into one cluster, which was confirmed by the experiment[25]. It is the reason that the isolation of single wall BNNT(9, 9) in aqueous solution is very difficult. With the assistance of polynucleotides, the number of cluster is more than one in all other systems. As seen in Fig. 9, the conformations of different systems at the end of 100 ns simulation were displayed. It assembled into 3 aggregates under the assistance of G_{15}, 4 aggregates under the assistance of A_{15}, 5 aggregates under the assistance of C_{15}, and 7 aggregates under the assistance of T_{15}, respectively. Especially in the system of MBNNT(9, 9)-T_{15}, 9 BNNT(9, 9) aggregated into 7 clusters. It strongly implicates that BNNT(9, 9) could disperse in aqueous solution under the assistance of polynucleotides, and the dispersion of BNNT(9, 9) could be affected by the wrapping manner of polynucleotides. As shown in Figure S2, it could be found that the base of polynucleotides is close to MBNNT(9, 9) surface, and phosphate group of polynucleotides prefer to interact with water

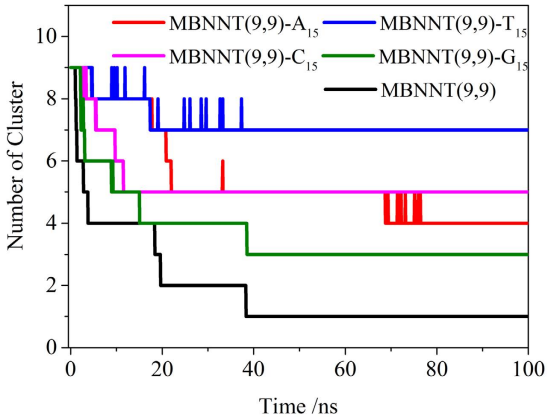

Figure 8. The change of number of cluster as a function of simulation time in the system of multiple BNNT(9, 9) in the solution of polynucleotides.

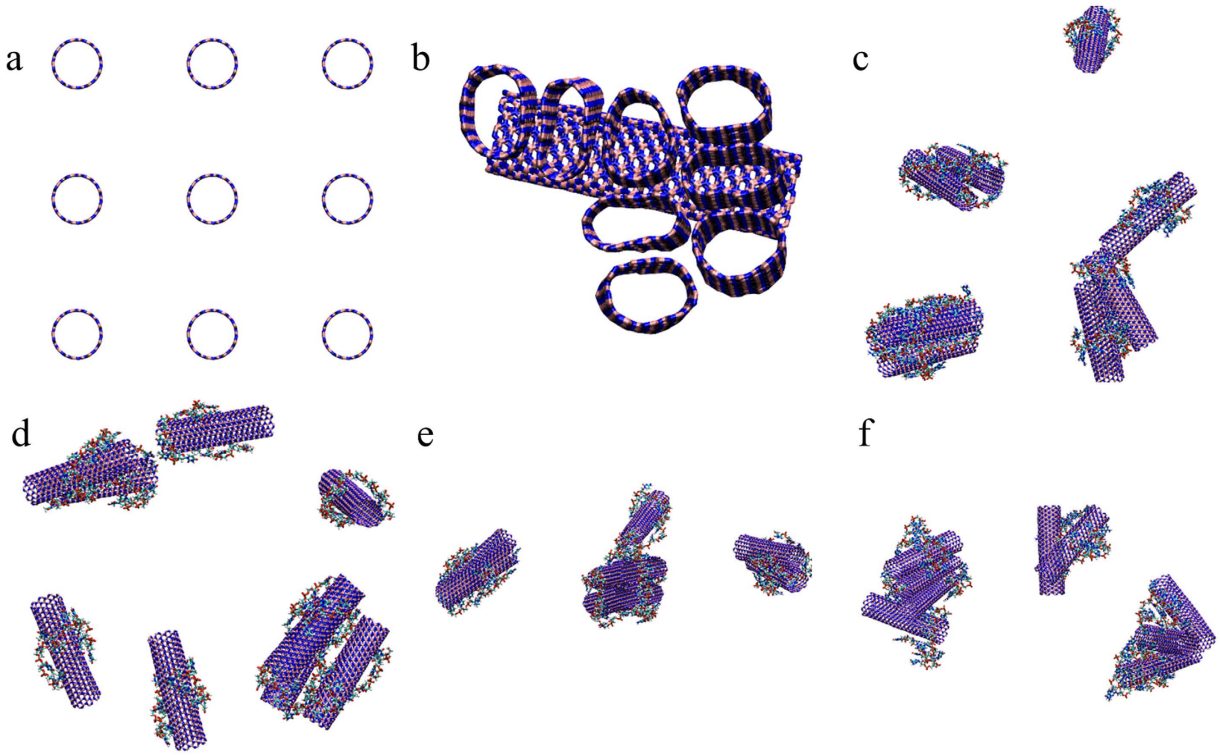

Figure 9. The snapshots of multiple BNNT(9, 9) in the simulation. The BNNTs and polynucleotides are represented by licorice model. (**a**) Initial structure of 9 BNNT(9, 9) in all systems; the last structure of 9 BNNT(9, 9) in the system of (**b**) MBNNT(9, 9), (**c**) MBNNT(9, 9)-A_{15}; (**d**) MBNNT(9, 9)-T_{15}; (**e**) MBNNT(9, 9)-C_{15}; (**f**) MBNNT(9, 9)-G_{15} in the simulation.

molecules. It mainly due to the fact that the negative charge of phosphate group could strongly interact with water molecules, and thus it could stabilize the dispersion of BNNT(9, 9) in aqueous. Especially, the number of cluster of MBNNT(9, 9) with T_{15} is 7. It indicate that BNNT(9, 9) with T_{15} could well disperse in aqueous solution. From the data of Fig. 5, the whole BNNT(9, 9) was circled by T_{15} through aromatic bases, and all phosphate groups of T_{15} is annularly distributed outside and interact with water molecules.

Effect of radius of BNNT on dispersion. To investigate the dispersion of BNNT by polynucleotides and the effect of radius of BNNT on dispersion, the MD simulation of systems with small radius of BNNT (BNNT(5, 5)) and polynucleotides (A_{15}, T_{15}, C_{15} and G_{15}) were performed. As seen in Figure S3, the BNNT(5, 5) could be wrapped by all polynucleotides (A_{15}, T_{15}, C_{15} and G_{15}). However, comparing with the wrapping of polynucleotides on BNNT(9, 9), not the whole circle of BNNT(5, 5) was surrounded by polynucleotides. It shows that the

	A	T
BNNT(5, 5)	64.02	67.78
BNNT(9, 9)	74.06	73.22

Table 2. The interaction between nucleotide and BNNTs (kJ/mol).

wrapping of polynucleotides on BNNT(9, 9) is much stronger than that of BNNT(5, 5). It could also be confirmed from the density distribution of phosphorus atoms of polynucleotides around BNNT (5, 5) in *x-y* plane, as seen in Figure S4. In addition, the aggregation process of 9 BNNT(5, 5) with polynucleotides in aqueous were observed. In Figure S5, the number of cluster of BNNT(5, 5) during the simulation was measured. The number of cluster of BNNT(5, 5) is 2 in both systems with A_{15} and T_{15}. It shows that 9 BNNT(5.5) aggregates in aqueous solution even with the assistance of polynucleotides. These results implicated that the strength of the interaction between polynucleotides and BNNT could certainly affect by the curvature of BNNT, and thus the dispersion of BNNT by polynucleotides is highly relate to the radius of BNNT.

The radius of BNNT(5, 5) is 0.35 nm, which is smaller than that of polynucleotides (~0.5 nm). The radius of BNNT(9, 9) is 0.62 nm, which is larger than that of polynucleotides. Therefore, the wrapping of polynucleotides on whole BNNT(5, 5) is more difficult than that on BNNT(9, 9). To understand the wrapping of nucleotides on BNNT from the view of adsorption energy, the interaction between single nucleotide (A and T) and BNNT including BNNT(5, 5) and BNNT(9, 9) was calculated by density functional theory (DFT), as shown in Table 2. The interaction between A and BNNT(5, 5) is around 64.02 kJ/mol, and it is 74.06 kJ/mol between A and BNNT(9, 9). The interaction between T and BNNT(5, 5) is around 67.78 kJ/mol, and it is 73.22 kJ/mol between A and BNNT(9, 9). It reveals that the interaction between nucleotides and BNNT(9, 9) is larger than that between nucleotides and BNNT(5, 5). It implicated that the radius of BNNT could affect the interaction between nucleotide and BNNT, and sequentially affects the wrapping of nucleotides on BNNT.

Conclusions

In summary, the molecular-level dispersion mechanism of BNNT in aqueous solution by polynucleotides was uncovered by molecular dynamics simulation. Our results showed that BNNT could be wrapped by polynucleotides in aqueous solution with the interaction between bases of polynucleotides and surface of BNNT. Polynucleotides have hydrophobic groups (base) and the hydrophilic groups (phosphate groups). The base of polynucleotides tends to closely interact with the surface of BNNT, and the phosphate atoms could interact with water molecules. Therefore, the phosphate groups of polynucleotides could assistant BNNT dispersing in aqueous and hinder the aggregation of BNNT. Meanwhile, the dispersion of BNNT in aqueous solution is greatly affected by the type of polynucleotides. Moreover, the radius of BNNT could also affect the dispersion of BNNT in aqueous solution by changing the interaction strength between nucleotides and BNNT. This work could help to understand the dispersion mechanism of BNNT in aqueous solution by the assistance of polynucleotides, and it may shade a light on the research of separation of single wall nanotubes by biomolecules.

References

1. Iijima, S. Helical microtubules of graphitic carbon. *Nature* **354,** 56–58 (1991).
2. Baughman, R. H., Zakhidov, A. A. & de Heer, W. A. Carbon nanotubes–the route toward applications. *Science* **297,** 787–792 (2002).
3. De Volder, M. F. L., Tawfick, S. H., Baughman, R. H. & Hart, A. J. Carbon nanotubes: present and future commercial applications. *Science* **339,** 535–539 (2013).
4. Cao, Q. *et al.* Arrays of single-walled carbon nanotubes with full surface coverage for high-performance electronics. *Nat. Nanotechnol.* **8,** 180–186 (2013).
5. Terrones, M. Carbon nanotubes: synthesis and properties, electronic devices and other emerging applications. *Int. Mater. Rev.* (2013).
6. Chopra, N. G., Luyken, R. J., Cherrey, K. & Crespi, V. H. Boron nitride nanotubes. *Science* **269,** 966 (1995).
7. Golberg, D., Bando, Y., Tang, C. C. & Zhi, C. Y. Boron nitride nanotubes. *Adv. Mater.* **19,** 2413–2432 (2007).
8. Golberg, D. *et al.* Boron nitride nanotubes and nanosheets. *ACS Nano* **4,** 2979–2993 (2010).
9. Ciofani, G., Raffa, V., Menciassi, A. & Cuschieri, A. Boron nitride nanotubes: an innovative tool for nanomedicine. *Nano Today* **4,** 8–10 (2009).
10. Siria, A. *et al.* Giant osmotic energy conversion measured in a single transmembrane boron nitride nanotube. *Nature* **494,** 455–458 (2013).
11. Nigues, A., Siria, A., Vincent, P., Poncharal, P. & Bocquet, L. Ultrahigh interlayer friction in multiwalled boron nitride nanotubes. *Nat. Mater.* **13,** 688–693 (2014).
12. Niskanen, J. *et al.* Boron nitride nanotubes as vehicles for intracellular delivery of fluorescent drugs and probes. *Nanomedicine* **11,** 447–463 (2016).
13. Fathalizadeh, A., Pham, T., Mickelson, W. & Zettl, A. Scaled synthesis of boron nitride nanotubes, nanoribbons, and nanococoons using direct feedstock injection into an extended-pressure, inductively-coupled thermal plasma. *Nano Lett.* **14,** 4881–4886 (2014).
14. Li, L. H., Cervenka, J., Watanabe, K., Taniguchi, T. & Chen, Y. Strong oxidation resistance of atomically thin boron nitride nanosheets. *ACS Nano* **8,** 1457–1462 (2014).
15. Wang, J. *et al.* Low temperature growth of boron nitride nanotubes on substrates. *Nano Lett.* **5,** 2528–2532 (2005).
16. Zhi, C. Y., Bando, Y., Tang, C. C., Huang, Q. & Golberg, D. Boron nitride nanotubes: functionalization and composites. *J. Mater. Chem.* **18,** 3900–3908 (2008).
17. Chang, C. W., Okawa, D., Majumdar, A. & Zettl, A. Solid-state thermal rectifier. *Science* **314,** 1121–1124 (2006).
18. Gao, Z., Zhi, C., Bando, Y., Golberg, D. & Serizawa, T. Noncovalent functionalization of disentangled boron nitride nanotubes with flavin mononucleotides for strong and stable visible-light emission in aqueous solution. *ACS Appl. Mater. Inter.* **3,** 627–632 (2011).
19. Park, C.-H. & Louie, S. G. Energy gaps and stark effect in boron nitride nanoribbons. *Nano Lett.* **8,** 2200–2203 (2008).
20. Ciofani, G., Raffa, V., Menciassi, A. & Cuschieri, A. Cytocompatibility, interactions, and uptake of polyethyleneimine-coated boron nitride nanotubes by living cells: Confirmation of their potential for biomedical applications. *Biotechnol. Bioeng.* **101,** 850–858 (2008).

21. Chen, X. *et al.* Boron nitride nanotubes are noncytotoxic and can be functionalized for interaction with proteins and cells. *J. Am. Chem. Soc.* **131,** 890–891 (2009).
22. Horvath, L. *et al. In vitro* investigation of the cellular toxicity of boron nitride nanotubes. *ACS Nano* **5,** 3800–3810 (2011).
23. Song, L. *et al.* Large scale growth and characterization of atomic hexagonal boron nitride layers. *Nano Lett.* **10,** 3209–3215 (2010).
24. Ciofani, G. *et al.* Boron nitride nanotubes: a novel vector for targeted magnetic drug delivery. *Curr. Nanosci.* **5,** 33–38 (2009).
25. Genchi, G. G. & Ciofani, G. Bioapplications of boron nitride nanotubes. *Nanomedicine* **10,** 3315–3319 (2015).
26. Khatti, Z. & Hashemianzadeh, S. M. Boron nitride nanotube as a delivery system for platinum drugs: Drug encapsulation and diffusion coefficient prediction. *Eur. J. Pharm. Sci.* **88,** 291–297 (2016).
27. Li, L. H. & Chen, Y. Atomically Thin Boron Nitride: Unique Properties and Applications. *Adv. Func. Mater.* **26,** 2594–2608 (2016).
28. Lee, C. H., Zhang, D. & Yap, Y. K. Functionalization, dispersion, and cutting of boron nitride nanotubes in water. *J. Phys. Chem. C* **116,** 1798–1804 (2011).
29. Gao, Z., Zhi, C., Bando, Y., Golberg, D. & Serizawa, T. Isolation of individual boron nitride nanotubes via peptide wrapping. *J. Am. Chem. Soc.* **132,** 4976–4977 (2010).
30. Zhi, C. *et al.* DNA-Mediated Assembly of Boron Nitride Nanotubes. *Chemistry–Asian J.* **2,** 1581–1585 (2007).
31. Mukhopadhyay, S., Gowtham, S., Scheicher, R. H., Pandey, R. & Karna, S. P. Theoretical study of physisorption of nucleobases on boron nitride nanotubes: a new class of hybrid nano-biomaterials. *Nanotechnology* **21,** 165703 (2010).
32. Gao, H. & Kong, Y. Simulation of DNA-nanotube interactions. *Annu. Rev. Mater. Res.* **34,** 123–150 (2004).
33. Liang, L., Chen, E.-Y., Shen, J.-W. & Wang, Q. Molecular modelling of translocation of biomolecules in carbon nanotubes: method, mechanism and application. *Mol. Sim.* **42,** 827–835 (2016).
34. Liang, L. *et al.* Charge-tunable insertion process of carbon nanotubes into DNA nanotubes. *J. Mol. Graph. Model.* **66,** 20–25 (2016).
35. Gao, H., Kong, Y., Cui, D. & Ozkan, C. S. Spontaneous insertion of DNA oligonucleotides into carbon nanotubes. *Nano Lett.* **3,** 471–473 (2003).
36. Shen, J.-W. *et al.* On the loading mechanism of ssDNA into carbon nanotubes. *RSC Adv.* **5,** 56896–56903, doi: 10.1039/C5RA01941A (2015).
37. Calvaresi, M. & Zerbetto, F. Atomistic molecular dynamics simulations reveal insights into adsorption, packing, and fluxes of molecules with carbon nanotubes. *J. Mater. Chem. A* **2,** 12123–12135 (2014).
38. Zhang, J. *et al.* Molecular recognition using corona phase complexes made of synthetic polymers adsorbed on carbon nanotubes. *Nat. Nanotechnol.* **8,** 959–968 (2013).
39. Zhang, Z.-S. *et al.* Peptide encapsulation regulated by the geometry of carbon nanotubes. *Biomaterials* **35,** 1771–1778 (2014).
40. Humphrey, W., Dalke, A. & Schulten, K. VMD: visual molecular dynamics. *J. Mol. Graph.* **14,** 33–38 (1996).
41. Froimowitz, M. HyperChem: a software package for computational chemistry and molecular modeling. *Biotechniques* **14,** 1010–1013 (1993).
42. Jorgensen, W. L., Chandrasekhar, J., Madura, J. D., Impey, R. W. & Klein, M. L. Comparison of simple potential functions for simulating liquid water. *J. Chem. Phys.* **79,** 926–935 (1983).
43. MacKerell, A. D. Jr. *et al.* All-atom empirical potential for molecular modeling and dynamics studies of proteins†. *J. Phys. Chem. B* **102,** 3586–3616 (1998).
44. Wu, Y., Wagner, L. K. & Aluru, N. R. Hexagonal boron nitride and water interaction parameters. *J. Chem. Phys.* **144,** 164118 (2016).
45. Darden, T., York, D. & Pedersen, L. Particle mesh Ewald: An N· log (N) method for Ewald sums in large systems. *J. Chem. Phys.* **98,** 10089–10092 (1993).
46. Kresse, G. & Furthmüller, J. Efficiency of ab-initio total energy calculations for metals and semiconductors using a plane-wave basis set. *Comp. Mater. Sci.* **6,** 15–50 (1996).
47. Blöchl, P. E. Projector augmented-wave method. *Phys. Rev. B* **50,** 17953 (1994).
48. Perdew, J. P., Burke, K. & Ernzerhof, M. Generalized gradient approximation made simple. *Phys. Rev. Lett.* **77,** 3865 (1996).
49. Henkelman, G., Uberuaga, B. P. & Jónsson, H. A climbing image nudged elastic band method for finding saddle points and minimum energy paths. *J. Chem. Phys.* **113,** 9901–9904 (2000).
50. Neugebauer, J. & Hess, B. A. Fundamental vibrational frequencies of small polyatomic molecules from density-functional calculations and vibrational perturbation theory. *J. Chem. Phys.* **118,** 7215–7225 (2003).
51. Kong, Z. *et al.* Charge-tunable absorption behavior of DNA on graphene. *J. Mater. Chem. B* **3,** 4814–4820 (2015).

Acknowledgements

We acknowledge financial support by the National Natural Science Foundation of China (Grant Nos 21674032, 21503186, 21403049), Zhejiang Provincial Natural Science Foundation of China (LY14B030008).

Author Contributions

J.S. and Z.Z. conceived the study, L.L. conducted the MD simulation and analysis, W.H. conducted the DFT calculation and analysis, L.L., W.H. and J.S. wrote the paper. All authors reviewed the manuscript.

Additional Information

Supplementary information accompanies this paper at http://www.nature.com/srep

Competing financial interests: The authors declare no competing financial interests.

How to cite this article: Liang, L. *et al.* Theoretic Study on Dispersion Mechanism of Boron Nitride Nanotubes by Polynucleotides. *Sci. Rep.* **6**, 39747; doi: 10.1038/srep39747 (2016).

Publisher's note: Springer Nature remains neutral with regard to jurisdictional claims in published maps and institutional affiliations.